Benefits and Development Challenges for Conversion-Alloying Anode Materials in Na-Ion Batteries

Amalie Skurtveit[1][*][†], Anders Brennhagen[1], Heesoo Park[1], Carmen Cavallo[1] and Alexey Y. Koposov[1,2][*]

[1]Centre for Material Science and Nanotechnology, Department of Chemistry, University of Oslo, Oslo, Norway, [2]Department of Battery Technology, Institute for Energy Technology (IFE), Kjeller, Norway
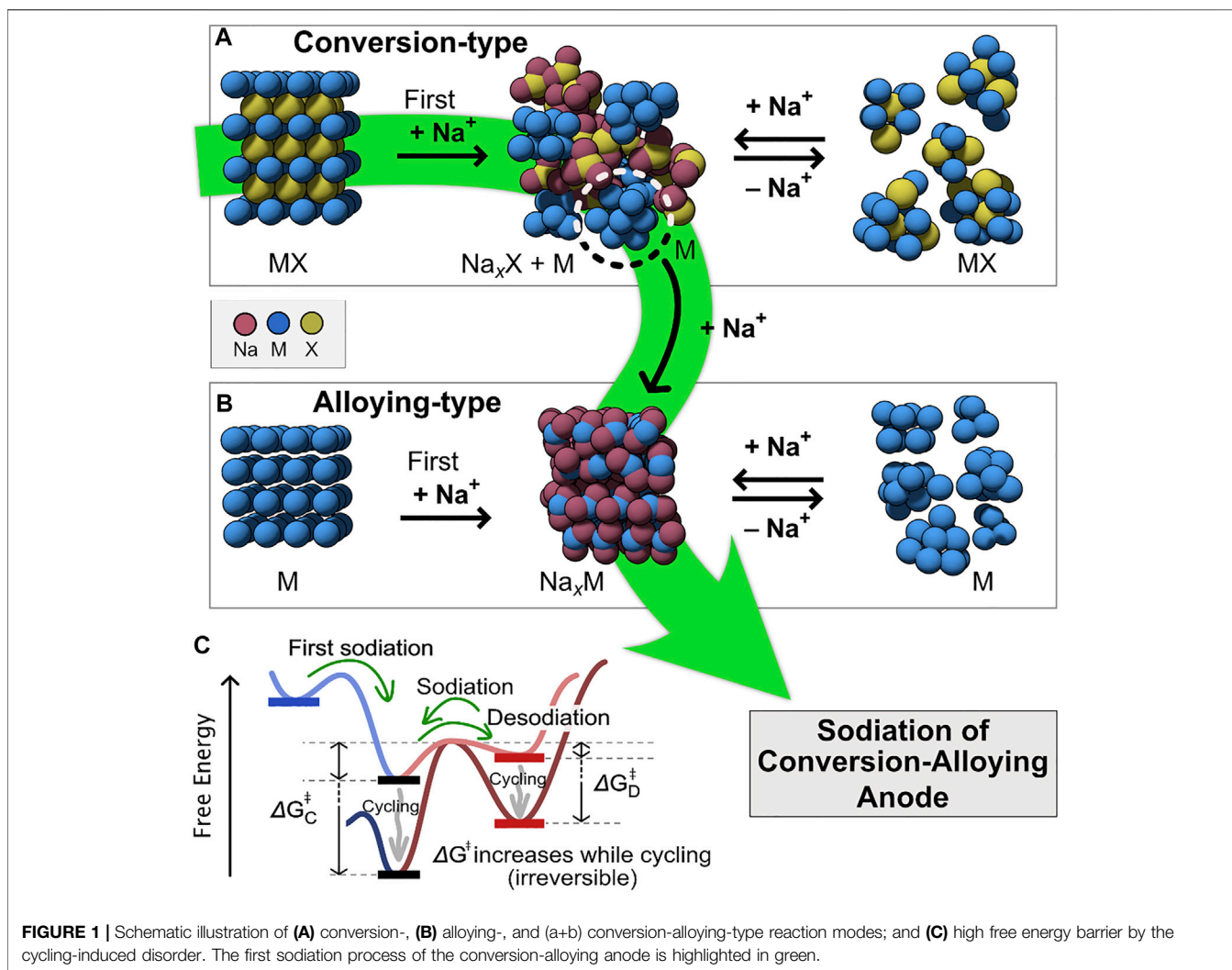
Over the past decade, Na-ion batteries (NIBs) have gained a substantial interest within the research community and relevant industry. NIBs are now emerging as a cost-effective and sustainable alternative to modern Li-ion batteries (LIBs). Similar to the parent LIB technology, NIB requires a new set of materials, which can boost battery capacity without sacrificing cycling stability, rate capabilities, and other performance targets. In NIB chemistry, anodes have received less attention compared to cathode chemistry, leaving hard carbon as a primary anode material, although its intercalation/adsorption mechanism limits the allowed number of Na-ions. Promising alternative groups of anodes are materials that undergo the combined conversion and alloying reactions (i.e., conversion-alloying anodes), due to the beneficial high theoretical capacity and good cycling stability. The conversion reaction in conversion-alloying anodes can be either reversible or irreversible, each possessing its advantages. However, the complexity of their operating mechanism(s) severely impedes their development. The present mini-review provides a survey of the recent developments of conversion-alloying-type anode materials for Na-ion batteries discussed in the context of their operation mechanism(s). Considering the chemical complexity of the conversion-alloying materials, the suggestions and guidance on characterization are provided along with theoretical considerations.

Keywords: sodium-ion batteries, conversion-alloying anodes, operando x-ray methods, (de)sodiation mechanism, *in situ* TEM, specific capacity, Na-ion batteries

INTRODUCTION

Na-ion batteries (NIBs) represent a cost-effective and sustainable alternative to Li-ion batteries (LIBs), promising for application in large-scale stationary energy storage systems (Vaalma et al., 2018; Hasa et al., 2021). While operating under the same rocking-chair principle as LIBs, the conventional anode materials used for LIBs, graphite and Si, are not suited for the use in NIBs (Moriwake et al., 2017; Zhang et al., 2017). Studies of hard carbon materials (most common anode material) are still in progress, but additional research efforts are focused on the other anode materials that follow different operating mechanisms, such as alloying and conversion (Wu et al., 2018; Usiskin et al., 2021; Zheng et al., 2021).
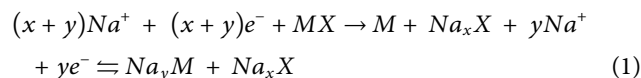
Conversion-based anode materials (**Figure 1A**) are mainly composed of transition metal oxides, sulfides, selenides, and phosphides, while elements from groups 14 and 15 (Si, Ge, Sn, P Sb, Bi, or binary alloys of these, e.g., BiSb, *etc.*) represent the most common alloying-based anode materials (**Figure 1B**)

FIGURE 1 | Schematic illustration of **(A)** conversion-, **(B)** alloying-, and (a+b) conversion-alloying-type reaction modes; and **(C)** high free energy barrier by the cycling-induced disorder. The first sodiation process of the conversion-alloying anode is highlighted in green.

(Zhang H. et al., 2018). Both the alloying- and the conversion-based materials exhibit high theoretical capacities ranging between 300-2000 mA h g^{-1} (Wang L. et al., 2019). However, as the chemical bonding structure and morphology constantly are altered during the (de)sodiation process (**Figures 1A,B**), both the conversion- and alloying-type anodes suffer from large volume expansion/contraction (Yao et al., 2017; Chen et al., 2019). This often leads to poor cycling stability (Tan et al., 2019; Wang L. et al., 2019; Fang et al., 2021; Villevieille, 2022). Moreover, before the (de)sodiation process reaches the final state, the varying intermediate alloy compositions are formed as crystalline (**Figure 1C**), of which metastability is determined within the energy of 70 meV/atom above the convex hull (ground state) (Sun et al., 2016). In addition, the mechanical stress by extensive volume variation limits the electronic contact and causes the electrode pulverization in the pure conversion and alloying process. Consequently, their thermodynamic change, which is caused by the kinetic factor after cycling, increases the free energy barrier and results in performance loss (Hudak et al., 2014; Huang et al., 2020).

Conversion-alloying materials (CAMs) offer a new strategy paving the diversity of available compounds for an innovative

anode material (Wang L. et al., 2019; Fang et al., 2021). CAMs can potentially deliver high specific capacities without the structural degradation mentioned above. Additionally, CAMs can also offer a reduction of the average working potential compared to pure conversion anodes and therefore increase the energy density in a full cell. CAMs combine the conversion and alloying mechanisms (**Figure 1, Eq. 1**).

$$
\begin{aligned}
(x + y)Na^+ &+ (x + y)e^- + MX \rightarrow M + Na_xX + yNa^+ \\
&+ ye^- \leftrightharpoons Na_yM + Na_xX
\end{aligned} \tag{1}
$$

The conversion reaction in these materials can be either reversible or irreversible. A reversible conversion reaction provides significantly higher capacities but suffers from the same problems as pure conversion reactions. Therefore, most studies on CAMs are with an irreversible conversion reaction and these will be the focus of this review. The initial irreversible conversion reaction results in the formation of electrochemically active nanoparticles dispersed within a matrix comprised of Na$_n$X (X = O, S, Se, Te, P, oxometallates). The formed active nanoparticles or clusters then participate in the reaction with

Na-ions through a reversible alloying mechanism. The formed matrix is capable of conducting Na-ions, and together with the active nanoparticles, which have high electronic conductivity, they secure a bi-continuous network beneficial for the electron- and Na$^+$-transport that translates into enhanced performance at high cycling rates (Kim et al., 2016; Durai et al., 2017; Lu et al., 2019). The beneficial role of entropy stabilization can be expected in enhancing the cycling performance of the anode during the redox phenomena (Wang Q. et al., 2019; Ghigna et al., 2020). The Na$_n$X matrix can accommodate the volumetric changes occurring during cycling and provide a physical separation between formed nanoparticles/clusters essentially prohibiting agglomeration/ electrochemical sintering of active components as well as particle pulverization. A good compromise between high capacity and cycling stability makes CAMs promising for implementation in next-generation NIBs.

CONVERSION-ALLOYING MATERIALS

CAMs must include an element that should be capable of alloying with Na-ions in its pure form. Therefore, CAMs for NIBs are based on elements from groups 14 or 15 (e.g., Ge, Sn, Sb, or Bi). CAMs require one or more elements that can participate in the conversion reaction, resulting in two classes: binary or ternary. Binary materials, primarily represented by Ge-, Sn-, Sb-, and Bi-based oxides, chalcogenides, and phosphides are the most investigated CAMs (Gu et al., 2013; Sottmann et al., 2016b; Li et al., 2019; Li C. C. et al., 2020; Wu et al., 2020; Shi et al., 2021). The oxides generally adopt a non-layered structure, while the chalcogenides tend to form layered structures due to the increased polarization of the electron cloud of the anions (Tan et al., 2019). In addition to the conversion and alloying reaction, the layered CAMs also include intercalation in the reaction mechanism. The performance of binary CAMs have been extensively reviewed elsewhere (Zhang H. et al., 2018; Fang et al., 2021).

Compared to binary CAMs, ternary materials are significantly less studied, however, several examples based on Bi- and Sb-based oxometallates of transition metals (BiFeO$_3$, Bi$_2$(MoO$_4$)$_3$, BiVO$_4$, Sb$_2$MoO$_6$, SbVO$_4$, Bi$_2$MoO$_6$) were reported (Durai et al., 2017; Sottmann et al., 2017; Lu et al., 2019; Pan et al., 2019; Brennhagen et al., 2022; Surendran et al., 2022). The choice of the second cation (Fe, Mo, V, etc.) is driven by the ability of the element to form a stable matrix without affecting gravimetric capacity. The large number of transition metals introduces the possibility to produce a variety of ternary CAMs.

The work reported by Sottmann et al., illustrates the benefits of CAMs by comparing three Bi-based anodes: Bi-metal, BiVO$_4$, and Bi$_2$(MoO$_4$)$_3$ (Sottmann et al., 2016a; Sottmann et al., 2017). Bi-metal had a high initial capacity (~500 mAh g^{-1}), rapidly decaying after 100 cycles to ~300 mAh g^{-1}. BiVO$_4$ and Bi$_2$(MoO$_4$)$_3$ showed stable capacities of ~350 mAh g^{-1} during the first 100 cycles. Sb$_2$MoO$_6$ exhibited stable capacities of ~ 600 mAh g^{-1} for 100 cycles when cycled at 200 mA g^{-1}, and 450 mAh g^{-1} for 450 cycles at 2 A g^{-1}. It also showed great rate capabilities maintaining the capacity of ~ 400 mAh g^{-1} cycled at

5 A g^{-1}, without any signs of significant degradation (Lu et al., 2019). However, recent studies on Sb$_2$MoO$_6$ have not been able to reproduce such incredible performances (Yang et al., 2019; Wu and Wang, 2020). Such discrepancies make the comparison between active materials difficult, not only because of the complexity of batteries in general, but also because of the number of choices for selecting other components of the electrodes. This can undermine materials' development because the materials themselves may have variations in chemical composition and different morphological features, surface chemistry, (nano)particle's sizes, and surface coatings that can substantially alter the electrochemical performance. The testing procedures of the materials (potential window, current density, temperature, etc.) are also different between studies, complicating the comparison of "equal" materials even more.
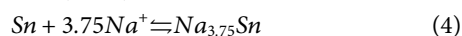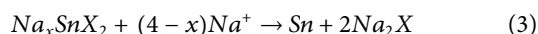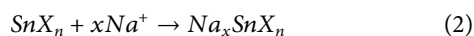
Nanostructuring techniques can generally improve the performance of CAMs, often applied in combination with carbon-based additives/coatings (Sottmann et al., 2016b; Sottmann et al., 2017; Wen et al., 2019; Dai et al., 2020), which is driven by the electrical conductivity. Many CAMs in their pristine state do not have high electronic conductivity, nor has the matrix formed through the conversion process. Creating nanosized CAMs mitigates the consequences of the volume change during the (de)sodiation processes and enhances their activity towards the conversion and alloying reaction (Poizot et al., 2000; Xu et al., 2016; Fang et al., 2019). This leads to a considerable reduction of the diffusion distance of Na-ions in the solid phase, which is beneficial for cycling stability and rate capability (Fang et al., 2021).

THE (DE)SODIATION MECHANISM

The rational design of CAMs is practically impossible without understanding the operating mechanism of CAMs. However, CAMs typically undergo a set of complex structural and chemical transformations during cycling (Fang et al., 2021). That often involves transformation through or into amorphous phases, which complicates the characterization of the materials. The "standard set" of electrochemical characterization techniques can aid in the overall understanding of the conversion-alloying mechanism, but other characterization techniques are also required. Due to complexity of the operating mechanism (i.e., formation of new phases, amorphization, etc.), post mortem and ex situ characterization techniques do not reveal the full scope of the reaction mechanisms. Additionally, air sensitivity and general instability of the materials after sodiation or metastable intermediates also represent a significant issue with ex situ characterization (Gao et al., 2018). Techniques such as operando X-ray diffraction (XRD), operando X-ray absorption spectroscopy (XAS), and in situ transmission electron microscopy (TEM) have emerged as suitable characterization techniques providing information complementary to the post mortem techniques. Worth mentioning that data-driven guidance is also considered as powerful tool to acquire in-

depth understanding of reaction processes and metastable intermediates (Bai et al., 2018). Mechanistic insights into the conversion-alloying reaction can be obtained by monitoring changes in both crystalline and amorphous phases, oxidation states of active elements, and local structure during (de)sodiation combined with structural modeling (Shadike et al., 2018; Cui et al., 2021a; Brennhagen et al., 2021).

For example, by applying *operando* XRD and *in situ* TEM it has been shown that layered Sn-chalcogenides (SnS$_2$ and SnSe$_2$) generally undergo through an intercalation step in addition to the conversion and alloying reactions (**Eqs 2–4**, respectively) (Shi et al., 2019; Liu et al., 2020; Zhang et al., 2020). *In situ* TEM have also been used to study other binary CAMs, and examples include Sb$_2$Se$_3$, Sb$_2$S$_3$, Sb$_2$Te$_3$/C Bi$_2$Te$_3$, SnO$_2$, and Sb$_2$Se$_3$/rGO (Gu et al., 2013; Ou et al., 2017; Yang et al., 2017; Yao et al., 2017; Wu et al., 2020; Cui et al., 2021b).

$$SnX_n + xNa^+ \rightarrow Na_xSnX_n \qquad (2)$$

$$Na_xSnX_2 + (4-x)Na^+ \rightarrow Sn + 2Na_2X \qquad (3)$$

$$Sn + 3.75Na^+ \rightleftharpoons Na_{3.75}Sn \qquad (4)$$

Upon sodiation of SnX$_n$ (X = S, Se), the intercalation of Na-ions 1) occur in the voltage range of ~ 2.5–1.1 V *vs.* Na/Na$^+$, followed by the conversion reaction 2) in the range 1.1–0.6 V *vs.* Na/Na$^+$, and the 1st cycle is finalized by the alloying reaction 3) in the 0.6–0.1 V region *vs.* Na/Na$^+$. Often, *in situ* TEM can be complementary to *operando* XRD, and *vice versa* (Ou et al., 2017).
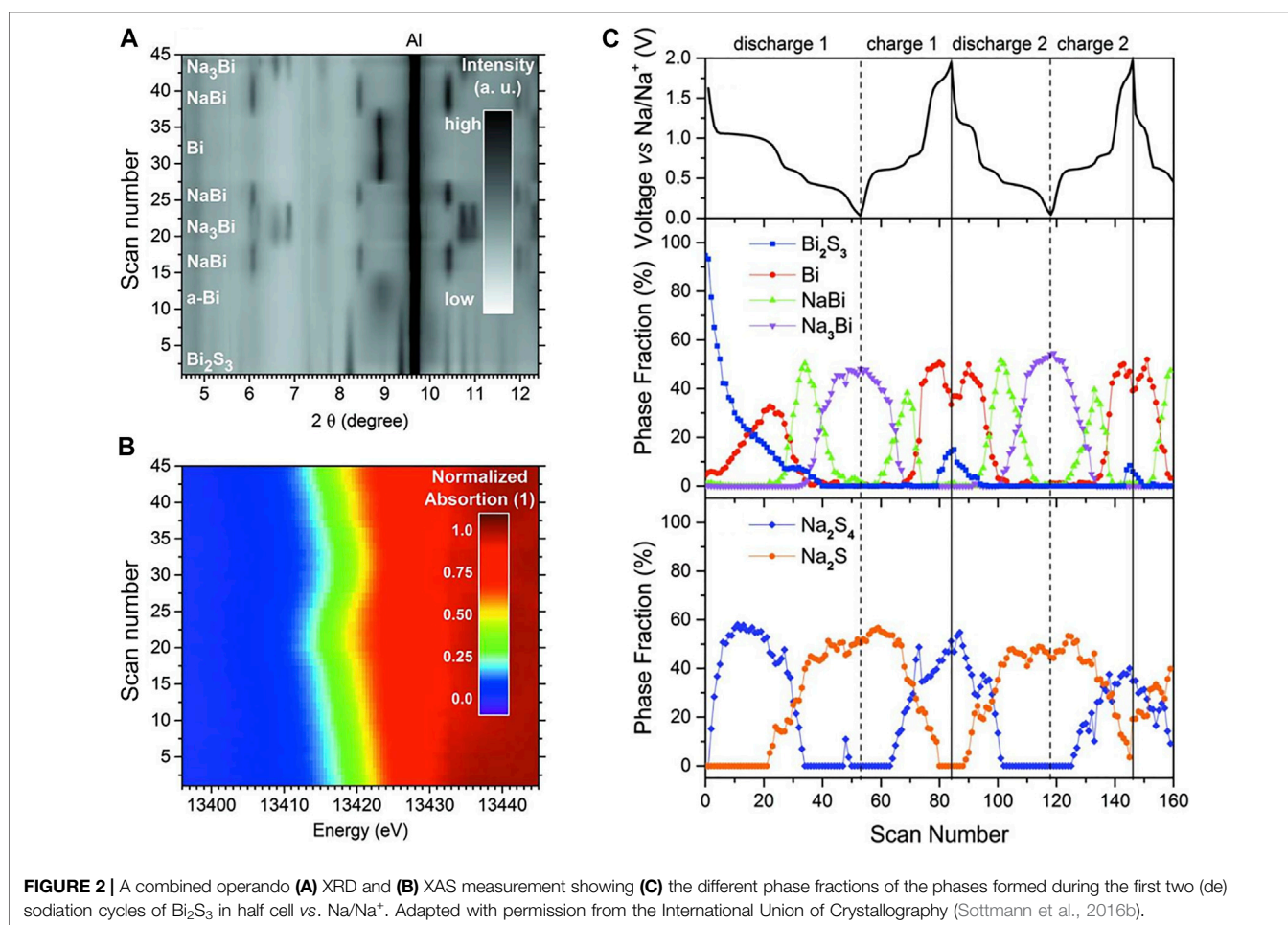
Operando XRD (due to its availability) is the most common characterization technique for assessment of the operation mechanism of CAMs (Brennhagen et al., 2021). *Operando* XRD has been used to elucidate the conversion and alloying reactions for binary CAM anodes (e.g., SnS$_2$, Bi$_2$S$_3$, Sb$_2$S$_3$ Sb$_2$O$_3$@ Sb, Sb$_2$O$_3$/rGO, Sb$_2$S$_3$@FeS$_2$, and Sb$_2$Se$_3$/rGO) (Sottmann et al., 2016b; Ou et al., 2017; Li et al., 2018; Ma et al., 2018; Shi et al., 2019; Cao et al., 2020). In many cases, (ternary CAMs) the matrix formed through the conversion is amorphous (Durai et al., 2017; Lu et al., 2019; Pan et al., 2019; Brennhagen et al., 2022), which calls for other characterization techniques to obtain an understanding of the operation mechanism. *Pair distribution function* (PDF) analysis is among such techniques allowing elucidating amorphous phases formed during (de)sodiation. However, to the best of our knowledge, no *operando* PDF has been performed on CAMs, while bulk Sb and Sn metal (a pure alloying anode) has been studied using *operando* PDF, showing that these relatively simple alloying reactions also contains amorphous intermediates (Allan et al., 2016; Stratford et al., 2017). This also means that we have more to learn from the alloying reactions in CAMs, even though the cycling mechanisms might seem quite clear when only using *operando* XRD.

Another useful *operando* technique, which is used to monitor specific elements in CAMs is *operando* XAS, where X-ray energies are scanned across the absorption edges of the target elements. This technique has been utilized to gain information on changes in oxidation states and local structures during cycling for Bi$_2$O$_3$, Bi$_2$S$_3$, BiVO$_4$, Bi$_2$(MoO$_4$)$_3$, SnO$_2$, and BiFeO$_3$ (Kim et al., 2016; Sottmann et al., 2016b; Sottmann et al., 2017; Dixon et al., 2019; Surendran et al., 2022). In the case of Bi$_2$S$_3$, a measurement combining *operando* XRD and XAS was used to reveal important aspects of the cycling mechanism (**Figure 2**) (Sottmann et al., 2016b). During the first sodiation, the irreversible conversion reaction forms amorphous Bi (wide and diffuse peak, **Figure 2A**) which further goes through a two-step alloying reaction into crystalline NaBi and Na$_3$Bi. A sharper peak for the Bi phase was observed after the first desodiation, indicating higher degree of crystallinity. The changes in the oxidation states of Bi are also linked to the edge shift in the XANES data (**Figure 2B**), showing that the oxidation state varies from Bi^{3+} in Bi$_2$S$_3$ to Bi^{3-} in Na$_3$Bi. The study further shows that the Na$_x$S matrix is not stable because it cycles between Na$_2$S$_4$ and Na$_2$S (**Figure 2C**). The conversion reaction is partially reversible because some Bi$_2$S$_3$ is retrieved at the end of the desodiation (**Figure 2C**), which is beneficial for specific capacity, but not practical for cycling stability (the second cycle demonstrates diminished formation of Bi$_2$S$_3$). Similar instabilities in the matrixes of some ternary CAMs, such as Bi$_2$MoO$_6$ and BiFeO$_3$, were observed (Brennhagen et al., 2022; Surendran et al., 2022). However, detailed studies on the behavior of the matrixes linked to the electrochemical performance are difficult to perform due to the complexity of the cycling mechanisms and species formed. As a result, such studies are limited and not always conclusive. This illustrates the importance of analysis of the matrix materials when working and designing CAMs.

DISCUSSION

There are clear indications that CAMs have significantly better cycling stability than the pure conversion or alloying materials, while still possessing higher capacities than intercalation materials. Variety of chemical compositions makes it possible to meet the desired compromise of high capacity, good cycling stability, cost, and environmental friendliness. There is a large playground for evaluation of alloying elements with transitions metals to produce ternary CAMs. Until present, only a few examples have been explored and there are more to discover in the future. Although the main general cycling mechanism is relatively well understood, the details of the mechanisms have only recently begun to unravel. The stability of the matrix is crucial to maintaining cycling stability and therefore deserves more research efforts. Meanwhile, the non-equilibrium phase of the nanoparticles formed through conversion is also relevant for materials design because co-existing phases (matrix) often exhibit and maintain extreme non-stoichiometry (Yao et al., 2017). There have been high-throughput search reports, along with the accelerated discovery efforts of promising anodes. However, due to the complicated electrochemical reaction with co-existing metastable phases in CAMs, the most high-throughput investigations of anodes have focused yet on single-phase mode within the limited length scale (Ong et al., 2011; Kirklin et al., 2013; Zhang X. et al., 2018; Zhang et al., 2019). This complexity makes CAMs challenging to study and develop. While CAM anodes emerge, it is critical to understand and classify the metastability of intermediate

FIGURE 2 | A combined operando **(A)** XRD and **(B)** XAS measurement showing **(C)** the different phase fractions of the phases formed during the first two (de) sodiation cycles of Bi_2S_3 in half cell vs. Na/Na⁺. Adapted with permission from the International Union of Crystallography (Sottmann et al., 2016b).

compounds for elements in the active anode's (de)sodiation reactions to provide data-driven guidance.

One of the biggest challenges with CAMs in full cells is the irreversible capacity loss during the first sodiation due to the irreversible conversion reaction. This demands that the cathode or electrolyte should supply more reaction Na-ions for the first discharge and could lead to a significant amount of dead mass for the subsequent cycles. This problem could be solved by presodiation. Even though this complicates the battery production, it could be viable due to the high capacity, good cycling stability, and rate performance that CAMs could potentially deliver. In addition, the design and optimization of the active element/matrix combination can also assist in mitigation of this complex challenge.

Estimation of the theoretical capacity of CAMs represents a challenge and requires a detailed understanding of the cycling mechanism, which involves multiple chemical and electrochemical transformations. Calculation of the theoretical capacity for CAMs is done by either assuming a fully reversible conversion and alloying reactions or assuming that only the alloying reaction contributes to the capacity. However, for several materials described above partially reversible conversion reactions and/or some electrochemical reactions in the matrix are commonly encountered, which complicate the

estimation of theoretical capacities. Such uncertainty, before determination of the operating mechanism makes it difficult to assess which reactions should be included in the calculated theoretical capacities. The 1-st cycle irreversible capacity (from the irreversible conversion reaction) combined with the SEI formation increases the gap between theoretical and measured specific capacity. It can still be useful to compare the theoretical capacity of certain stages of the reactions to the specific capacities of the corresponding plateaus in the (de)sodiation curves to improve the understanding of the reaction mechanisms.

Considering the abovementioned complication, it is very important to provide all the necessary details of the study and do comparative studies to get a clearer picture of the actual performance of the material as was emphasized in a few recent publications (Li J. et al., 2020; Stephan, 2021; Sun, 2021). The experimental uncertainties add to the complexity of the problem for assessment of the specific vs. theoretical capacities of CAMs. That includes proper consideration of other components of the electrodes, potentially uneven distribution of active material on the electrode sheet, proper statistics of the results, and accurate measurement of the mass of the active material. The latter can deliver an error of $\geq 10\%$ to the calculated specific capacity when performed at the laboratory scale (Brennhagen et al., 2022). In addition, specific current densities rather than C-rates should be preferably reported when working with

these materials, as a determination of the C-rate requires an accurate estimation of the theoretical capacity.

In conclusion, CAMs, while yet underexplored and poorly understood deliver a large potential for the future of NIBs, however, their challenges and operating mechanisms have to be properly examined. That requires not only synthetic efforts, but also careful consideration of the electrochemical characterization techniques as well as development and selection of the *operando* tools.

AUTHOR CONTRIBUTIONS

AS: conceptualization, main writing, reviewing, and editing, literature study. AB: conceptualization, writing, reviewing, and editing. HP: conceptualization, writing, reviewing, editing, and visualization. CC: conceptualization, writing, reviewing, and editing. AK: conceptualization, writing, reviewing, and editing.

FUNDING

REFERENCES

Allan, P. K., Griffin, J. M., Darwiche, A., Borkiewicz, O. J., Wiaderek, K. M., Chapman, K. W., et al. (2016). Tracking Sodium-Antimonide Phase Transformations in Sodium-Ion Anodes: Insights from Operando Pair Distribution Function Analysis and Solid-State NMR Spectroscopy. *J. Am. Chem. Soc.* 138 (7), 2352–2365. doi:10.1021/jacs.5b13273

Bai, Q., Yang, L., Chen, H., and Mo, Y. (2018). Computational Studies of Electrode Materials in Sodium-Ion Batteries. *Adv. Energ. Mater.* 8 (17), 1702998. doi:10.1002/aenm.201702998

Brennhagen, A., Cavallo, C., Wragg, D. S., Sottmann, J., Koposov, A. Y., and Fjellvåg, H. (2021). Understanding the (De)Sodiation Mechanisms in Na-Based Batteries through Operando X-ray Methods. *Batteries & Supercaps* 4 (7), 1039–1063. doi:10.1002/batt.202000294

Brennhagen, A., Cavallo, C., Wragg, D. S., Vajeeston, P., Sjåstad, A. O., Koposov, A. Y., et al. (2022). Operando XRD Studies on Bi2MoO6 as Anode Material for Na-Ion Batteries. *Nanotechnology* 33 (18), 185402. doi:10.1088/1361-6528/ac4eb5

Cao, L., Gao, X., Zhang, B., Ou, X., Zhang, J., and Luo, W.-B. (2020). Bimetallic Sulfide Sb2S3@FeS2 Hollow Nanorods as High-Performance Anode Materials for Sodium-Ion Batteries. *ACS Nano* 14 (3), 3610–3620. doi:10.1021/acsnano.0c00020

Chen, W., Zhang, X., Mi, L., Liu, C., Zhang, J., Cui, S., et al. (2019). High-Performance Flexible Freestanding Anode with Hierarchical 3D Carbon-Networks/F27S8/Graphene for Applicable Sodium-Ion Batteries. *Adv. Mater.* 31 (8), 1806664. doi:10.1002/adma.201806664

Cui, J., Zheng, H., and He, K. (2021a). *In Situ* TEM Study on Conversion-Type Electrodes for Rechargeable Ion Batteries. *Adv. Mater.* 33 (6), 2000699. doi:10.1002/adma.202000699

Cui, J., Zheng, H., Zhang, Z., Hwang, S., Yang, X.-Q., and He, K. (2021b). Origin of Anomalous High-Rate Na-Ion Electrochemistry in Layered Bismuth telluride Anodes. *Matter* 4 (4), 1335–1351. doi:10.1016/j.matt.2021.01.005

Dai, S., Wang, L., Shen, Y., and Wang, M. (2020). Bismuth Selenide Nanocrystalline Array Electrodes for High-Performance Sodium-Ion Batteries. *Appl. Mater. Today* 18, 100455. doi:10.1016/j.apmt.2019.100455

Dixon, D., Ávila, M., Ehrenberg, H., and Bhaskar, A. (2019). Difference in Electrochemical Mechanism of SnO2 Conversion in Lithium-Ion and Sodium-Ion Batteries: Combined in Operando and *Ex Situ* XAS Investigations. *ACS Omega* 4 (6), 9731–9738. doi:10.1021/acsomega.9b00563

Durai, L., Moorthy, B., Issac Thomas, C., Kyung Kim, D., and Kamala Bharathi, K. (2017). Electrochemical Properties of BiFeO3 Nanoparticles: Anode Material for Sodium-Ion Battery Application. *Mater. Sci. Semiconductor Process.* 68, 165–171. doi:10.1016/j.mssp.2017.06.003

Fang, L., Bahlawane, N., Sun, W., Pan, H., Xu, B. B., Yan, M., et al. (2021). Conversion-Alloying Anode Materials for Sodium Ion Batteries. *Small* 17 (37), 2101137. doi:10.1002/smll.202101137

Fang, Y., Yu, X.-Y., and Lou, X. W. (2019). Nanostructured Electrode Materials for Advanced Sodium-Ion Batteries. *Matter* 1 (1), 90–114. doi:10.1016/j.matt.2019.05.007

Gao, H., Ma, W., Yang, W., Wang, J., Niu, J., Luo, F., et al. (2018). Sodium Storage Mechanisms of Bismuth in Sodium Ion Batteries: An Operando X-ray Diffraction Study. *J. Power Sourc.* 379, 1–9. doi:10.1016/j.jpowsour.2018.01.017

Ghigna, P., Airoldi, L., Fracchia, M., Callegari, D., Anselmi-Tamburini, U., D'Angelo, P., et al. (2020). Lithiation Mechanism in High-Entropy Oxides as Anode Materials for Li-Ion Batteries: An Operando XAS Study. *ACS Appl. Mater. Inter.* 12 (45), 50344–50354. doi:10.1021/acsami.0c13161

Gu, M., Kushima, A., Shao, Y., Zhang, J.-G., Liu, J., Browning, N. D., et al. (2013). Probing the Failure Mechanism of SnO2 Nanowires for Sodium-Ion Batteries. *Nano Lett.* 13 (11), 5203–5211. doi:10.1021/nl402633n

Hasa, I, Mariyappan, S., Saurel, D., Adelhelm, P., Koposov, A. Y., Masquelier, C., et al. (2021). Challenges of Today for Na-Based Batteries of the Future: From Materials to Cell Metrics. *J. Power Sourc.* 482, 228872. doi:10.1016/j.jpowsour.2020.228872

Huang, Y.-X., Wu, F., and Chen, R.-J. (2020). Thermodynamic Analysis and Kinetic Optimization of High-Energy Batteries Based on Multi-Electron Reactions. *Natl. Sci. Rev.* 7 (8), 1367–1386. doi:10.1093/nsr/nwaa075

Hudak, N. S., Davis, L. E., and Nagasubramanian, G. (2014). Cycling-Induced Changes in the Entropy Profiles of Lithium Cobalt Oxide Electrodes. *J. Electrochem. Soc.* 162 (3), A315–A321. doi:10.1149/2.0071503jes

Kim, M.-K., Yu, S.-H., Jin, A., Kim, J., Ko, I.-H., Lee, K.-S., et al. (2016). Bismuth Oxide as a High Capacity Anode Material for Sodium-Ion Batteries. *Chem. Commun.* 52 (79), 11775–11778. doi:10.1039/C6CC06712C

Kirklin, S., Meredig, B., and Wolverton, C. (2013). High-Throughput Computational Screening of New Li-Ion Battery Anode Materials. *Adv. Energ. Mater.* 3 (2), 252–262. doi:10.1002/aenm.201200593

Li, C. C., Wang, B., Chen, D., Gan, L.-Y., Feng, Y., Zhang, Y., et al. (2020a). Topotactic Transformation Synthesis of 2D Ultrathin GeS2 Nanosheets toward High-Rate and High-Energy-Density Sodium-Ion Half/Full Batteries. *ACS Nano* 14 (1), 531–540. doi:10.1021/acsnano.9b06855

Li, H., Qian, K., Qin, X., Liu, D., Shi, R., Ran, A., et al. (2018). The Different Li/Na Ion Storage Mechanisms of Nano Sb2O3 Anchored on Graphene. *J. Power Sourc.* 385, 114–121. doi:10.1016/j.jpowsour.2018.03.031

Li, J., Arbizzani, C., Kjelstrup, S., Xiao, J., Xia, Y.-y., Yu, Y., et al. (2020b). Good Practice Guide for Papers on Batteries for the Journal of Power Sources. *J. Power Sourc.* 452, 227824. doi:10.1016/j.jpowsour.2020.227824

Li, W., Li, X., Liao, J., Zhao, B., Zhang, L., Liu, Y., et al. (2019). Structural Design of Ge-Based Anodes with Chemical Bonding for High-Performance Na-Ion Batteries. *Energ. Storage Mater.* 20, 380–387. doi:10.1016/j.ensm.2019.04.034

Liu, Z., Daali, A., Xu, G.-L., Zhuang, M., Zuo, X., Sun, C.-J., et al. (2020). Highly Reversible Sodiation/Desodiation from a Carbon-Sandwiched SnS2 Nanosheet Anode for Sodium Ion Batteries. *Nano Lett.* 20 (5), 3844–3851. doi:10.1021/acs.nanolett.0c00964

Lu, X., Wang, Z., Liu, K., Luo, J., Wang, P., Niu, C., et al. (2019). Hierarchical Sb2MoO6 Microspheres for High-Performance Sodium-Ion Battery Anode. *Energ. Storage Mater.* 17, 101–110. doi:10.1016/j.ensm.2018.11.021

Ma, W., Wang, J., Gao, H., Niu, J., Luo, F., Peng, Z., et al. (2018). A Mesoporous Antimony-Based Nanocomposite for Advanced Sodium Ion Batteries. *Energ. Storage Mater.* 13, 247–256. doi:10.1016/j.ensm.2018.01.016

Moriwake, H., Kuwabara, A., Fisher, C. A. J., and Ikuhara, Y. (2017). Why Is Sodium-Intercalated Graphite Unstable? *RSC Adv.* 7 (58), 36550–36554. doi:10.1039/C7RA06777A

Ong, S. P., Chevrier, V. L., Hautier, G., Jain, A., Moore, C., Kim, S., et al. (2011). Voltage, Stability and Diffusion Barrier Differences between Sodium-Ion and Lithium-Ion Intercalation Materials. *Energy Environ. Sci.* 4 (9), 3680–3688. doi:10.1039/C1EE01782A

Ou, X., Yang, C., Xiong, X., Zheng, F., Pan, Q., Jin, C., et al. (2017). A New rGO-Overcoated Sb2Se3 Nanorods Anode for Na+Battery: *In Situ* X-Ray Diffraction Study on a Live Sodiation/Desodiation Process. *Adv. Funct. Mater.* 27 (13), 1606242. doi:10.1002/adfm.201606242

Pan, J., Zhang, Y., Li, L., Cheng, Z., Li, Y., Yang, X., et al. (2019). Polyanions Enhance Conversion Reactions for Lithium/Sodium-Ion Batteries: The Case of SbVO 4 Nanoparticles on Reduced Graphene Oxide. *Small Methods* 3 (10), 1900231. doi:10.1002/smtd.201900231

Poizot, P., Laruelle, S., Grugeon, S., Dupont, L., and Tarascon, J.-M. (2000). Nano-sized Transition-Metal Oxides as Negative-Electrode Materials for Lithium-Ion Batteries. *Nature* 407 (6803), 496–499. doi:10.1038/35035045

Shadike, Z., Zhao, E., Zhou, Y. N., Yu, X., Yang, Y., Hu, E., et al. (2018). Advanced Characterization Techniques for Sodium-Ion Battery Studies. *Adv. Energ. Mater.* 8 (17), 1702588. doi:10.1002/aenm.201702588

Shi, X., Chen, S. L., Fan, H. N., Chen, X. H., Yuan, D., Tang, Q., et al. (2019). Metallic-State SnS 2 Nanosheets with Expanded Lattice Spacing for High-Performance Sodium-Ion Batteries. *ChemSusChem* 12 (17), 4046–4053. doi:10.1002/cssc.201901355

Shi, X., Liu, W., Xue, H., Chen, B., Wang, C., Sun, L., et al. (2021). An Exploration on the Improvement of Reversible Conversion and Capacity Retention of Sb2O3-Based Anode Materials for Alkali Metal-Ion Storage by Fe-C Co-hybridization. *J. Power Sourc.* 506, 230074. doi:10.1016/j.jpowsour.2021.230074

Sottmann, J., Herrmann, M., Vajeeston, P., Hu, Y., Ruud, A., Drathen, C., et al. (2016a). How Crystallite Size Controls the Reaction Path in Nonaqueous Metal Ion Batteries: The Example of Sodium Bismuth Alloying. *Chem. Mater.* 28 (8), 2750–2756. doi:10.1021/acs.chemmater.6b00491

Sottmann, J., Herrmann, M., Vajeeston, P., Ruud, A., Drathen, C., Emerich, H., et al. (2017). Bismuth Vanadate and Molybdate: Stable Alloying Anodes for Sodium-Ion Batteries. *Chem. Mater.* 29 (7), 2803–2810. doi:10.1021/acs.chemmater.6b04699

Sottmann, J., Homs-Regojo, R., Wragg, D. S., Fjellvåg, H., Margadonna, S., and Emerich, H. (2016b). Versatile Electrochemical Cell for Li/Na-Ion Batteries and High-Throughput Setup for combined operando X-ray Diffraction and Absorption Spectroscopy. *J. Appl. Cryst.* 49 (6), 1972–1981. doi:10.1107/S160057671601428X

Stephan, A. K. (2021). Standardized Battery Reporting Guidelines. *Joule* 5 (1), 1–2. doi:10.1016/j.joule.2020.12.026

Stratford, J. M., Mayo, M., Allan, P. K., Pecher, O., Borkiewicz, O. J., Wiaderek, K. M., et al. (2017). Investigating Sodium Storage Mechanisms in Tin Anodes: A Combined Pair Distribution Function Analysis, Density Functional Theory, and Solid-State NMR Approach. *J. Am. Chem. Soc.* 139 (21), 7273–7286. doi:10.1021/jacs.7b01398

Sun, W., Dacek, S. T., Ong, S. P., Hautier, G., Jain, A., Richards, W. D., et al. (2016). The Thermodynamic Scale of Inorganic Crystalline Metastability. *Sci. Adv.* 2 (11), e1600225. doi:10.1126/sciadv.1600225

Sun, Y.-K. (2021). An Experimental Checklist for Reporting Battery Performances. *ACS Energ. Lett.* 6 (6), 2187–2189. doi:10.1021/acsenergylett.1c00870

Surendran, A., Enale, H., Thottungal, A., Sarapulova, A., Knapp, M., Nishanthi, S. T., et al. (2022). Unveiling the Electrochemical Mechanism of High-Capacity Negative Electrode Model-System BiFeO3 in Sodium-Ion Batteries: An in Operando XAS Investigation. *ACS Appl. Mater. Inter.* 14, 7856–7868. doi:10.1021/acsami.1c20717

Tan, H., Chen, D., Rui, X., and Yu, Y. (2019). Peering into Alloy Anodes for Sodium-Ion Batteries: Current Trends, Challenges, and Opportunities. *Adv. Funct. Mater.* 29 (14), 1808745. doi:10.1002/adfm.201808745

Usiskin, R., Lu, Y., Popovic, J., Law, M., Balaya, P., Hu, Y.-S., et al. (2021). Fundamentals, Status and Promise of Sodium-Based Batteries. *Nat. Rev. Mater.* 6 (11), 1020–1035. doi:10.1038/s41578-021-00324-w

Vaalma, C., Buchholz, D., Weil, M., and Passerini, S. (2018). A Cost and Resource Analysis of Sodium-Ion Batteries. *Nat. Rev. Mater.* 3 (4), 18013. doi:10.1038/natrevmats.2018.13

Villevieille, C. (2022). Interfaces and Interphases in Batteries: How to Identify and Monitor Them Properly Using Surface Sensitive Characterization Techniques. *Adv. Mater. Inter* 9, 2101865. doi:10.1002/admi.202101865

Wang, L., Światowska, J., Dai, S., Cao, M., Zhong, Z., Shen, Y., et al. (2019a). Promises and Challenges of alloy-type and Conversion-type Anode Materials for Sodium-Ion Batteries. *Mater. Today Energ.* 11, 46–60. doi:10.1016/j.mtener.2018.10.017

Wang, Q., Sarkar, A., Wang, D., Velasco, L., Azmi, R., Bhattacharya, S. S., et al. (2019b). Multi-anionic and -cationic Compounds: New High Entropy Materials for Advanced Li-Ion Batteries. *Energ. Environ. Sci.* 12 (8), 2433–2442. doi:10.1039/C9EE00368A

Wen, S., Zhao, J., Zhao, Y., Xu, T., and Xu, J. (2019). Reduced Graphene Oxide (RGO) Decorated Sb2S3 Nanorods as Anode Material for Sodium-Ion Batteries. *Chem. Phys. Lett.* 716, 171–176. doi:10.1016/j.cplett.2018.12.031

Wu, C., Dou, S. X., and Yu, Y. (2018). The State and Challenges of Anode Materials Based on Conversion Reactions for Sodium Storage. *Small* 14 (22), 1703671. doi:10.1002/smll.201703671

Wu, Q., and Wang, H. G. (2020). Sb2MoO6 Decorated on Graphene as an Anode Material for Lithium/Sodium-Ion Batteries. *J. Phys. Conf. Ser.* 1605 (1), 012176. doi:10.1088/1742-6596/1605/1/012176

Wu, Y., Luo, W., Gao, P., Zhu, C., Hu, X., Qu, K., et al. (2020). Unveiling the microscopic origin of asymmetric phase transformations in (de)sodiated Sb2Se3 with *In Situ* transmission electron microscopy. *Nano Energy* 77, 105299. doi:10.1016/j.nanoen.2020.105299

Xu, Y., Zhou, M., and Lei, Y. (2016). Nanoarchitectured Array Electrodes for Rechargeable Lithium- and Sodium-Ion Batteries. *Adv. Energ. Mater.* 6 (10), 1502514. doi:10.1002/aenm.201502514

Yang, L., Liao, H., Tian, W., Hong, W., Cai, P., Liu, C., et al. (2019). Rod-Like Sb2MoO6: Structure Evolution and Sodium Storage for Sodium-Ion Batteries. *Small Methods* 3 (5), 1800533. doi:10.1002/smtd.201800533

Yang, Z., Sun, J., Ni, Y., Zhao, Z., Bao, J., and Chen, S. (2017). Facile Synthesis and *In Situ* Transmission Electron Microscopy Investigation of a Highly Stable Sb2Te3/C Nanocomposite for Sodium-Ion Batteries. *Energ. Storage Mater.* 9, 214–220. doi:10.1016/j.ensm.2017.07.010

Yao, S., Cui, J., Lu, Z., Xu, Z.-L., Qin, L., Huang, J., et al. (2017). Unveiling the Unique Phase Transformation Behavior and Sodiation Kinetics of 1D van der Waals Sb2S3 Anodes for Sodium Ion Batteries. *Adv. Energ. Mater.* 7 (8), 1602149. doi:10.1002/aenm.201602149

Zhang, F., Shen, Y., Shao, M., Zhang, Y., Zheng, B., Wu, J., et al. (2020). SnSe2 Nanoparticles Chemically Embedded in a Carbon Shell for High-Rate Sodium-Ion Storage. *ACS Appl. Mater. Inter.* 12 (2), 2346–2353. doi:10.1021/acsami.9b16659

Zhang, H., Hasa, I., and Passerini, S. (2018a). Beyond Insertion for Na-Ion Batteries: Nanostructured Alloying and Conversion Anode Materials. *Adv. Energ. Mater.* 8 (17), 1702582. doi:10.1002/aenm.201702582

Zhang, L., Hu, X., Chen, C., Guo, H., Liu, X., Xu, G., et al. (2017). In Operando Mechanism Analysis on Nanocrystalline Silicon Anode Material for Reversible and Ultrafast Sodium Storage. *Adv. Mater.* 29 (5), 1604708. doi:10.1002/adma.201604708

Zhang, X., Zhang, Z., Yao, S., Chen, A., Zhao, X., and Zhou, Z. (2018b). An Effective Method to Screen Sodium-Based Layered Materials for Sodium Ion Batteries. *Npj Comput. Mater.* 4 (1), 13. doi:10.1038/s41524-018-0070-2

Zhang, Z., Zhang, X., Zhao, X., Yao, S., Chen, A., and Zhou, Z. (2019). Computational Screening of Layered Materials for Multivalent Ion Batteries. *ACS Omega* 4 (4), 7822–7828. doi:10.1021/acsomega.9b00482

Zheng, S.-M., Tian, Y.-R., Liu, Y.-X., Wang, S., Hu, C.-Q., Wang, B., et al. (2021). Alloy Anodes for Sodium-Ion Batteries. *Rare Met.* 40 (2), 272–289. doi:10.1007/s12598-020-01605-z

Conflict of Interest: The authors declare that the research was conducted in the absence of any commercial or financial relationships that could be construed as a potential conflict of interest.

Publisher's Note: All claims expressed in this article are solely those of the authors and do not necessarily represent those of their affiliated organizations, or those of the publisher, the editors and the reviewers. Any product that may be evaluated in this article, or claim that may be made by its manufacturer, is not guaranteed or endorsed by the publisher.